

Cell Injury, Repair, Aging and Apoptosis

Stromal Cell-Derived Factor-1 Is Essential for Photoreceptor Cell Protection in Retinal Detachment

Hiroki Otsuka,* Noboru Arimura,* Shozo Sonoda,* Makoto Nakamura,† Teruto Hashiguchi,‡ Ikuro Maruyama,‡ Shintaro Nakao,§ Ali Hafezi-Moghadam,§ and Taiji Sakamoto*

From the Departments of Ophthalmology, and Laboratory and Vascular Medicine,‡ Kagoshima University Graduate School of Medical and Dental Sciences, Kagoshima, Japan; the Division of Ophthalmology,† the Department of Surgery, Kobe University Graduate School of Medicine, Kobe, Japan; and the Angiogenesis Laboratory,§ Massachusetts Eye and Ear Infirmary, the Department of Ophthalmology, Harvard Medical School, Boston, Massachusetts*

Stromal cell-derived factor-1 (SDF-1) causes chemotaxis of CXCR4-expressing bone marrow-derived cells. SDF-1 is involved in the pathogenesis of various vascular diseases, including those of the eye. However, the role of SDF-1 in neuronal diseases is not completely understood. Here, we show higher SDF-1 levels in the vitreous humor of patients with retinal detachment (RD) compared with normal patients. SDF-1 correlated positively with the duration as well as the extent of RD. Furthermore, SDF-1 correlated significantly with levels of interleukin-6 and interleukin-8, but not with vascular endothelial growth factor. Western blot analysis results showed significant SDF-1 up-regulation in detached rat retinas compared with normal animals. Immunohistochemistry data showed that SDF-1 was co-localized with the glial cells of the detached retina. SDF-1 blockade with a neutralizing antibody increased photoreceptor cell loss and macrophage accumulation in the subretinal space. The retinal precursor cell line R28 expressed CXCR4. SDF-1 rescued serum starvation-induced apoptosis in R28 cells and enhanced their ability to participate in wound closure in a scratch assay. Our results indicate a surprising, protective role for SDF-1 in RD. This effect may be mediated directly or indirectly through other cell types. (*Am J Pathol* 2010, 177:2268–2277; DOI: 10.2353/ajpath.2010.100134)

Chemokines are a family of polypeptides that act as potent chemoattractants. They are structurally grouped

into two subfamilies, CXC-family and CC- subfamily, based on the characteristic presence of four conserved cysteine residues.^{1–3} Stromal cell-derived factor-1 (SDF-1) is a CXC-chemokine with important roles in hematopoiesis.⁴ Mice lacking SDF-1 or its receptor CXCR4 are embryonically lethal, exhibiting defects in various organs including heart, brain, large vessels, and bone marrow.^{5,6} In bone marrow, endothelial cells and stromal cells express SDF-1, which not only recruits hematopoietic stem cells to the bone marrow niche, but also supports their survival and proliferation.^{7,8} SDF-1/CXCR4 also recruits bone marrow-derived cells to neovascularization and regeneration sites in heart, liver,^{9,10} and eye.^{11,12}

SDF-1 levels are elevated in the vitreous of ischemic ocular diseases, such as proliferative diabetic retinopathy (PDR) and retinopathy of prematurity.^{12,13} Previously, we reported elevated vitreous levels of SDF-1 in patients with retinal vein occlusion.¹⁴ In addition, SDF-1/CXCR4 potentially mediates ocular inflammation by recruiting CD4⁺ T-cells, and is potentially involved in the formation of proliferative membranes in eyes with proliferative vitreoretinopathy.^{15,16} Therefore, interest in understanding the role of SDF-1/CXCR4 in non-neovascular inflammatory or proliferative ocular diseases remains great.

Retinal detachment (RD), the physical separation of the neural layer of the retina from the subjacent retinal pigment epithelium, results in photoreceptor cell death.^{17,18} Because of the irreversible nature of the damage, a long duration of RD can cause permanent vision loss.¹⁹ Thus, new insights into the photoreceptor protection in RD would be of great clinical interest, as they could lead to new treatments. Because, the retina is an acces-

Supported in part by a grant from the Research Committee on Chorioretinal Degeneration and Optic Atrophy, Ministry of Health, Labor, and Welfare (T.S.), and by a Grant-in-Aid for Scientific Research (number 20390450) from the Ministry of Education, Science, and Culture of the Japanese Government.

Accepted for publication June 24, 2010.

CME Disclosure: None of the authors disclosed any relevant financial relationships.

Address reprint requests to Taiji Sakamoto, M.D., Ph.D., Department of Ophthalmology, Kagoshima University Graduate School of Medical and Dental Sciences, 8-35-1, Sakuragaoka, Kagoshima, 890-8520, Japan. E-mail: tsakamot@m3.kufm.kagoshima-u.ac.jp.

sible part of the brain, it also offers a unique opportunity for studies of the central nervous system. Given that RD usually occurs without infectious inflammation or destructive ischemia, it provides a suitable context for investigating morphological changes in neural disorders and a local sterile inflammation.

The CC chemokine monocyte chemoattractant protein-1, erythropoietin, and interleukin (IL)-6 have recently been implicated in neuro protection.^{20,21} Monocyte chemoattractant protein-1 is a critical mediator of RD-induced photoreceptor apoptosis.²²

This study elucidates the role of SDF-1 in RD by using human vitreous samples *in vivo* and *in vitro*.

Materials and Methods

Human Vitreous Samples

This study was approved by the institutional ethical committee at University of Kagoshima, and was performed in accordance with the Declaration of Helsinki. All surgeries were performed at Kagoshima University Hospital. All patients provided informed consent before receiving treatment. Undiluted vitreous fluid samples (0.5 to 0.7 ml) were obtained from the same sites of the anterior vitreous by pars plana vitrectomy. Vitreous humor was collected in sterile tubes, placed immediately on ice, centrifuged to remove cells and debris, and stored at -80°C until analysis. The clinical histories of all patients were obtained from their medical records. In patients with rhegmatogenous RD (RRD), preoperative data collection included time from onset of symptoms to surgery and extent of detached retina.

Measurements of vitreous levels of SDF-1 α , vascular endothelial growth factor (VEGF), and inflammatory cytokines/chemokines (IL-1 β , IL-6, IL-8, IL-10, IL-12p70, and tumor necrosis factor- α) were measured as we described previously.²³ SDF-1 α and VEGF were quantified by using commercial enzyme-linked immunosorbent assays (Human CXCL12/SDF-1 α Quantikine ELISA Kit, Human VEGF Quantikine ELISA Kit; R&D Systems, Minneapolis, MN). Six inflammatory cytokines/chemokines were quantified by using commercial multiplex Cytometric Bead Array systems: Human Inflammation Kit (BD Biosciences Pharmingen, San Diego, CA). All concentrations less than the detection level were assigned a value of 0 in the subsequent analysis.

Animals and RD Induction

All experiments were performed in accordance with the Association for Research in Vision and Ophthalmology statement for the Use of Animals in Ophthalmic and Vision Research and approval of our institutional animal care committee. Brown Norway rats (Kyudo, Fukuoka, Japan), postnatal 8 weeks, were studied as follows. RD was induced in the right eyes as we described previously.²³ The rats were anesthetized with an intramuscular injection of ketamine and xylazine, and their pupils were dilated with topical 1% tropicamide and 2.5% phenylephrine hydrochloride. The retinas were detached by using a subretinal injection

of 1% sodium hyaluronate (Opegan; Santen, Osaka, Japan) with an anterior chamber puncture to reduce intraocular pressure. Sclera was penetrated at the ocular nasal equator with a 30-Gauge needle. Then, sodium hyaluronate (0.05 ml) was gently injected through the sclera into the subretinal space to enlarge the RDs. These procedures were performed only in the right eye, with the left eye serving as a control. Eyes with lens injury, vitreous hemorrhage, infection, and spontaneous reattachment were excluded from the analysis.

Intravitreal Injection

In some eyes, immediately after RD induction, 1 μg anti-SDF-1 α antibody (MAB310; R&D Systems) or 1 μg isotype control IgG1 monoclonal antibody (MAB002; R&D Systems) was injected intravitreally from the temporal limbus of the same eye by using a 33-Gauge needle (Hamilton, Reno, NV) in a 10- μl volume. Doses were based on previous studies in mice.²⁴ The rats were sacrificed on days 3 and 7 after treatment, and the eyes were harvested for study.

Western Blot Analysis of Experimental RD

SDF-1 expression in the detached retinas was examined by Western blot, as described previously.²⁵ The rats were sacrificed 3 days after RD induction. The eyes were enucleated immediately, and the anterior segment and vitreous were removed. The detached portion of the neurosensory retina was carefully peeled and harvested. Retinas were resuspended in lysis buffer (30 mmol/L Tris, pH 7.5, 150 mmol/L NaCl, 1 mmol/L phenylmethylsulfonyl fluoride, 1 mmol/L Na₃VO₄, 1% Nonidet P-40, and 10% glycerol), and centrifuged for 10 minutes at 4°C. Protein concentration in the supernatant was calculated by using the micro bicinchoninic acid protein assay kit (Pierce, Rockford, IL). An aliquot of 50 μg total extract was mixed with protein loading buffer containing methoxyethanol, and boiled for 5 minutes before being loaded onto 15% SDS-polyacrylamide gels, then transferred onto a polyvinylidene difluoride membrane. The membrane was blocked by incubation with blocking buffer (Tris-buffered saline [pH 7.5] with 5% nonfat dry milk and 0.1% Tween-20) for 1 hour at room temperature. The membrane was then incubated with rabbit polyclonal anti-SDF-1 α antibody (1:1000; Abcam, Cambridge, UK) at 4°C overnight. The blots were subsequently probed with secondary anti-rabbit antibodies conjugated to horseradish peroxidase, and images were developed by using the enhanced chemiluminescence system plus (GE Health care, Tokyo, Japan).

Immunofluorescent Staining

The eyes were fixed in 4% paraformaldehyde at 4°C overnight. The anterior segment and the lens were removed, and the remaining eye cup was cryoprotected with 10% to 30% sucrose in PBS. The eye cups were then frozen in an optimal cutting temperature compound (Sakura Finetech, Tokyo, Japan). Frozen sections (8 μm) were dried and

blocked with blocking buffer for 1 hour. The antibodies used for staining were rabbit polyclonal anti-SDF-1 α antibody, rabbit polyclonal anti-CXCR4 antibody (each 1:50; Abcam), monoclonal anti-gial fibrillary acidic protein (GFAP) antibody (Sigma, St. Louis, MO), mouse anti-CD68 monoclonal antibody (ED1; 1:800; Serotec, Raleigh, NC), and mouse anti-CD31 monoclonal antibody (PECAM-1; 1:100; Abcam). Normal rabbit or mouse IgG was used instead of primary antibody as a negative control in each case. Secondary antibodies were Alexa-Fluor 488-conjugated goat anti-mouse IgG F(ab)₂ fragment and Alexa-Fluor 594-conjugated goat anti-rabbit IgG F(ab)₂ fragment (each 1:400; Molecular Probes, Carlsbad, CA). Slides were counterstained with 4,6-diamidino-2-phenylindole (DAPI), mounted with Shandon PermaFlour (Thermo Scientific, Waltham, MA), and viewed with a Olympus fluorescence microscope (Olympus, Tokyo, Japan). Images were captured by using the same exposure time for each comparative section. Confocal Laser Scanning Microscopy images were taken on an Olympus FV-500 confocal microscope (Olympus). For all experiments, at least three sections from each eye were evaluated.

Immunofluorescent staining for CXCR4 was performed on R28 cells by using the same method.

Quantification of Outer Nuclear Layer Thickness and ED1 Positive Macrophages

To evaluate the change of outer nuclear layer (ONL) thickness after RD, we compared the thickness of the ONL with the entire retina (defined as the distance between the internal limiting membrane to the external limiting membrane) in histological sections (three sections each point) stained with hematoxylin and eosin. Three separate measurements of retinal thickness were obtained from each retinal section by using image analysis software, Image J (National Institutes of Health, Bethesda, MD). To assess the number of ED1 positive macrophages infiltrating the subretinal space, we performed double immune-fluorescence staining with rabbit polyclonal anti-CXCR4 antibody and ED1. The number of ED1 positive cells was counted at three random fields in each eye in a masked fashion.

Cell Culture

The rat immortalized retinal precursor cell line R28, a gift from Dr. G. M. Siegel (The State University of New York, Buffalo), was cultured in Dulbecco's modified Eagle's medium high glucose supplemented with 10% fetal bovine serum, 10 mmol/L nonessential amino acids, and 10 mg/ml gentamicin as described previously.²⁶ Cells were incubated at 37°C in a 5% CO₂ incubator and subcultured with 0.05% trypsin-EDTA. Subconfluent cultures were trypsinized and seeded for the following experiments.

Trypan Blue Dye Exclusion Assay

To induce cell death by serum starvation, R28 cells at 50% confluence in 24-well tissue culture plates were

washed with PBS twice, and the culture medium was replaced with serum-free Dulbecco's modified Eagle's medium containing 0.1% bovine serum albumin. After 6 hours of synchronization, recombinant SDF-1 α (Pepro-Tech, London, UK) or PBS was added to the wells at the indicated concentrations. After incubation for 48 hours, cell survival was assessed by trypan blue dye exclusion assay in a masked fashion, as described previously.²⁷

Terminal Deoxynucleotidyl Transferase-Mediated dUTP Nick-End Labeling Staining

Terminal deoxynucleotidyl transferase-mediated dUTP nick-end labeling (TUNEL) procedure and quantification of TUNEL-positive cells were performed by using an ApopTag fluorescein direct *in situ* apoptosis detection kit (Chemicon International, Temecula, CA) according to the manufacturer's instructions. The number of TUNEL-positive cells was counted in a masked fashion.

Scratch Wound Assay

For scratch wound assay, R28 cells were grown to 90% confluence in 6-well tissue culture plates and serum starved for 6 hours before experiment. Then, R28 cells were scratched with a sterile 0.1- to 10- μ l pipette tip (TipOne; USA Scientific, Ocala, FL) to remove cells with three parallel linear scrapes. The debris of damaged cells was removed by washing, and the cells were refed with serum-free Dulbecco's modified Eagle's medium containing 0.1% bovine serum albumin in the presence or absence of recombinant (rSDF-1) (100 ng/ml). The progression of wound healing was photographed immediately and 24 hours after wounding, at the same field near the marked point, using an inverted microscope (Olympus CKX41; Olympus) equipped with a digital camera. The extent of healing is defined as the ratio of the area difference between the original wound and the remaining wound 24 hours after injury compared with the original wound.²⁸ The wound area was determined by the number of pixels in histogram (Photoshop CS3; Adobe, San Jose, CA).

Western Blot Analysis of Bcl-2 or ERK-1/2 Activation

R28 cells (5×10^5) were subcultured on 6-cm tissue culture dishes. The cells were serum-starved for 6 hours and then stimulated with or without rSDF-1 (100 ng/ml) for 24 hours.²⁹ For inhibition studies, U0126 (Promega, Madison, WI) was added 1 hour before SDF-1 treatment. In brief, whole cells were lysed with SDS sample buffer and a 80- μ g volume of protein extracts was loaded onto 15% SDS-polyacrylamide gels, then transferred onto a polyvinylidene difluoride membrane. After blocking, the membrane was reacted with anti-Bcl-2 antibody (1:1000; Cell Signaling Technology, Beverly, MA) at 4°C overnight. The blots were subsequently probed with secondary antibodies and images were developed. To analyze activation of ERK-1/2, the membrane was reacted with phospho-ERK-

Table 1. Patient Characteristics

Characteristics	PDR	RRD	ERM	MH	P
Subjects, no.	30	44	11	18	
Age (yr)	62 (31–80)	59 (44–86)	69 (50–75)	68 (49–78)	0.184*
Female sex no. (%)	15 (50)	18 (41)	6 (55)	11 (61)	0.849†

Values are expressed as the median (range) or number (%).

*Kruskal-Wallis variance analysis.

† χ^2 test.

1/2 (1:1000; Cell Signaling Technology). After detection of phospho-ERK-1/2, the blot was stripped and re-probed with an antibody against total ERK-1/2 (1:1000; Cell Signaling Technology), as described previously.³⁰

Statistical Analysis

The vitreous inflammatory cytokine/chemokine concentrations in each group were compared by using the Mann-Whitney *U*-test. The correlation between inflammatory cytokines/chemokines in RD samples was analyzed by using a simple linear regression analysis and Spearman's rank correlation coefficient. All *in vitro* and *in vivo* data are presented as mean \pm SEM, and the significance of differences between groups was determined by Student's *t*-test. *P* values less than 0.05 were considered significant.

Results

Vitreous SDF-1 and Inflammatory Cytokine/Chemokine Levels in Patients with RD, Epiretinal Membrane, and Macular Hole

To investigate the role of SDF-1 in non-neovascular ocular diseases, we quantified the levels of human vitreous SDF-1 in RRD, epiretinal membrane (ERM), and macular hole (MH). PDR, a neovascular disease with high levels of SDF-1 in the vitreous, was used as a positive control.³¹ Samples were harvested from 30 eyes with PDR, 44 eyes with RRD, 11 eyes with ERM, and 18 eyes with MH. There were no statistically significant differences in age and sex of patients (Table 1).

SDF-1 concentration of RRD (58.5 pg/ml) was significantly higher than that of ERM (21.2 pg/ml, $P = 0.012$ and $P < 0.016$ after Bonferroni correction). Significant differences were not found between RRD and MH (10.0 pg/ml), or between MH and ERM (Figure 1A). The vitreous VEGF level in PDR was highest and comparable to that of SDF-1. In contrast, there was surprisingly no VEGF detectable in RRD, ERM, and MH (Figure 1B).

Next, we examined whether there is a relation between vitreous SDF-1 concentration and pathological condition in eyes with RRD, in terms of duration of disease (range, 3 to 120 days) and extent of detached retina (range, 0.5 to 4 quadrants; Table 2). The vitreous SDF-1 level in RRD was positively correlated with duration of disease and extent of detached retina in RRD by a simple linear regression ($r = 0.501$, $P < 0.001$, $r = 0.339$, $P = 0.024$, respectively) and by a Spearman's rank correlation coef-

ficient ($r = 0.347$, $P = 0.025$, $r = 0.323$, $P = 0.040$, respectively; Figure 1, C and D).

Furthermore, vitreous SDF-1 showed a positive correlation with IL-6 ($r = 0.484$, $P = 0.002$) and IL-8 ($r = 0.400$, $P = 0.009$) by Spearman's rank correlation coefficient (Figure 1, E and F), but not by simple linear regression. The vitreous IL-6 in RRD positively correlated with the extent of detached retina by a Spearman's rank correlation coefficient ($r = 0.342$, $P = 0.027$; data not shown); however, it did not correlate with disease duration.

SDF-1 and CXCR4 Expression in Experimental RD

To investigate SDF-1 and CXCR4 expression in the retina after RD, 3 days after detachment was induced in Brown Norway rats, neurosensory retina was harvested and expression of these proteins was analyzed by Western blotting. The SDF-1 protein level in the detached retina was substantially higher ($P < 0.01$), 3 days after RD, compared with the untreated control (Figure 2, A and B).

Immunofluorescent staining revealed sparse SDF-1 expression in the inner border and the outer plexiform layer of the retina in the control. In contrast, up-regulation of the expression of SDF-1 occurred with RD (Figure 3, A and B), which seemed to be colocalized with the activated GFAP-positive astrocytes or Müller cells (Figure 3, C–F).

In the normal retina, CXCR4 staining mainly was present in the ganglion cell layer and the inner nuclear layer of the retina. Additionally, CXCR4 was strongly positive in the outer nuclear layer and photoreceptor inner segments of the detached retina (Figure 4, A–D). Double immunofluorescent staining of CXCR4 showed strong staining in some ED-1-positive macrophages infiltrating into the subretinal space (Figure 5, A–C).

Vitreous SDF-1 Neutralization Causes ONL Cell Loss and Accumulation of Subretinal ED-1 Positive Macrophages

To further define the role of SDF-1 in RD, after sodium hyaluronate injection into the subretinal space, some rats were intravitreally injected with anti-SDF-1 antibody or nonbinding control antibody. Three days after RD, there were no apparent morphological differences between the Ab-injected animals and normal controls. Seven days after RD, there was thinning of the outer nuclear layer due

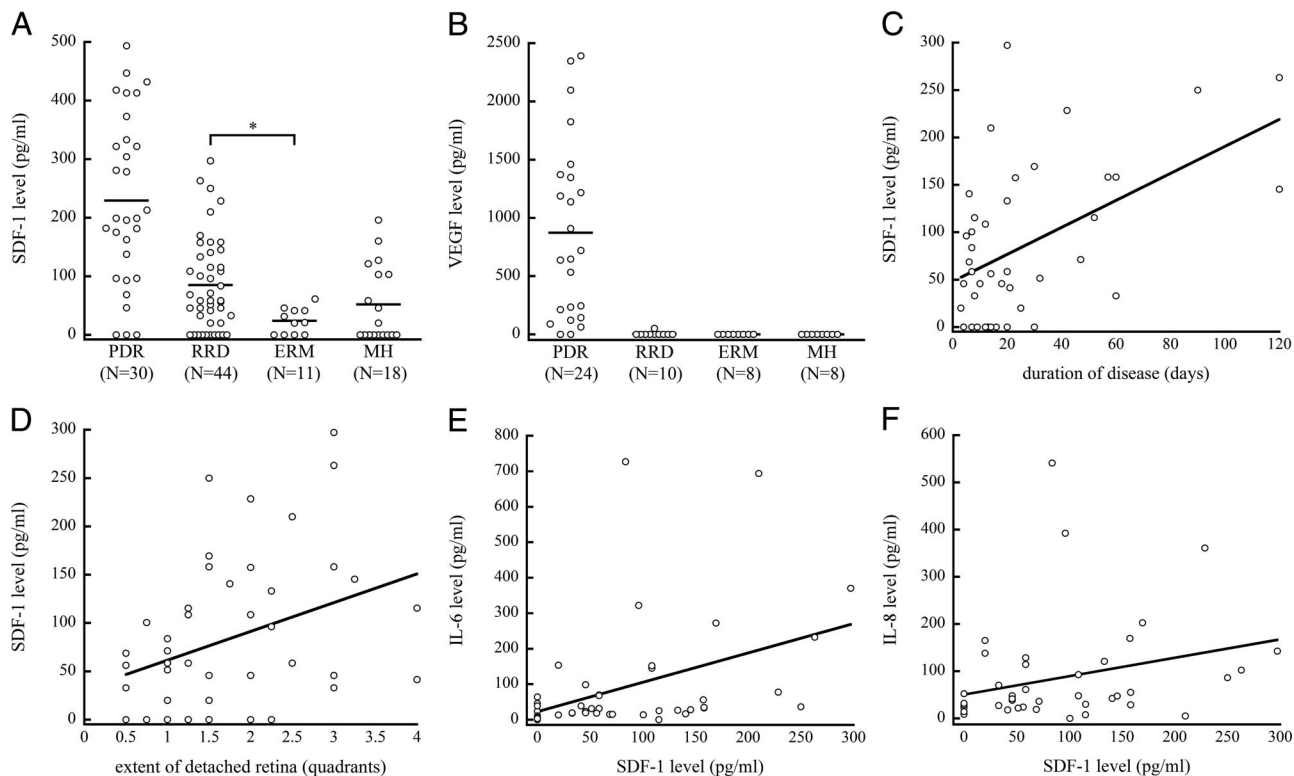


Figure 1. Analysis of human vitreous levels of SDF-1. **A:** Vitreous levels of PDR, RRD, ERM, and MH. The vitreous SDF-1 level of RRD was significantly higher than that of ERM. Bars indicate average values. **B:** Vitreous levels of VEGF. **C** and **D:** Scatter plot for the correlation between vitreous levels of SDF-1 and **(C)** duration of disease (simple linear regression, $r = 0.501$, $P < 0.001$; Spearman's rank correlation coefficient, $r = 0.347$, $P = 0.025$) or **(D)** extent of detached retina (simple linear regression, $r = 0.339$, $P = 0.024$; Spearman's rank correlation coefficient, $r = 0.323$, $P = 0.040$) in eyes with RRD. **E** and **F:** Scatter plot for the correlation between vitreous levels of SDF-1 and **(E)** IL-6 (simple linear regression, $r = 0.410$, $P = 0.006$; Spearman's rank correlation coefficient, $r = 0.484$, $P = 0.002$) or **(F)** IL-8 duration of disease (simple linear regression, $r = 0.081$, $P = 0.061$; Spearman's rank correlation coefficient, $r = 0.400$, $P = 0.009$) in eyes with RRD.

to photoreceptor loss and deconstruction of the inner and outer segments of the photoreceptors. The ratio of the thickness of the ONL to the entire retina differed significantly between the noninjected (0.278 ± 0.015) and anti-SDF-1 Ab group (0.228 ± 0.011 , $P < 0.05$), or between anti-SDF-1 Ab and control Ab group (0.294 ± 0.018 , $P < 0.01$), respectively. No significant difference was found between noninjected and control Ab group (Figure 6, A and B). In normal eyes without detachment, SDF-1 blockade did not cause apparent retinal morphological change (data not shown). This suggests that SDF-1 blockade results in photoreceptor cell loss only at the site of detachment.

TUNEL staining of rat eyes 3 days after detachment revealed significantly higher percentages of TUNEL-positive cells in the ONL of retinas treated with anti-SDF-1 Ab compared with those treated with control Ab ($P < 0.05$) or untreated control ($P < 0.05$; Figure 6, C and D).

To assess the impact of SDF-1 blockade on the recruitment of inflammatory cells, the number of infiltrated mac-

rophages was counted after immunostaining with ED-1. The number of ED-1 positive macrophages that infiltrated the subretinal space was markedly increased in anti-SDF-1 Ab group, compared with both noninjected ($P < 0.05$) and control Ab group ($P < 0.05$; Figure 6, E and F).

SDF-1/CXCL12 Enhances R28 Survival and Apoptosis

To assess whether SDF-1 is a survival factor for retinal cells, we performed *in vitro* experiments with R28 cells, a

Table 2. Clinical State of Rhegmatogenous Retinal Detachment

Duration of disease (days)	15 (3–120)
Extent of detached retina (quadrants)	1.5 (0.5–4)

Values are expressed as the median (range).

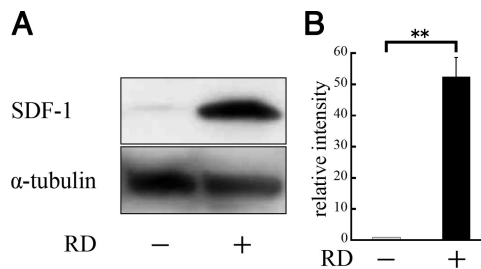


Figure 2. Western blot analysis of SDF-1 protein expression in retinas of normal rats and 3 days after detachment. Experimental retinal detachment was created by injection of sodium hyaluronate. The neurosensory retina was harvested and analyzed by Western blotting. **A:** Immunoreactive band for SDF-1 in rat retinal tissue with or without detachment. **B:** Quantification of the relative SDF-1 expression ($n = 3$). Results are the mean \pm SEM. $**P < 0.01$.

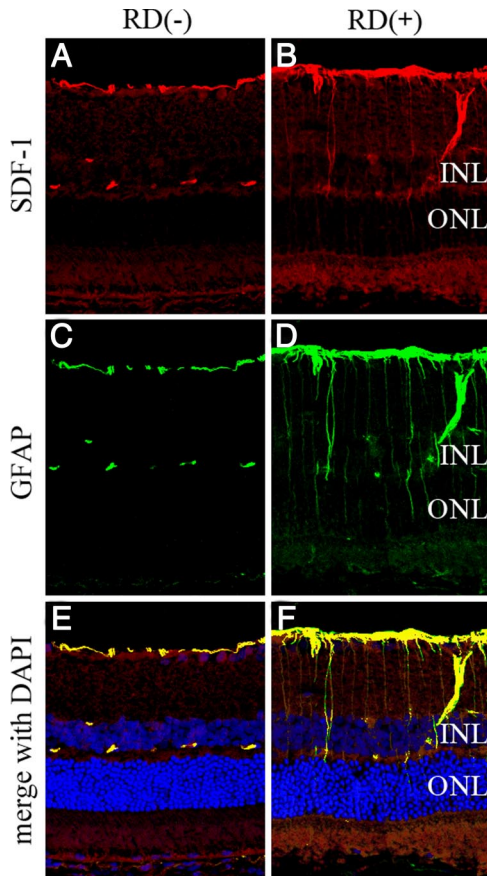


Figure 3. Confocal images of SDF-1 expression in detached rat retina. Retinal sections from control eyes (**A**, **C**, and **E**) or 3 days after detachment (**B**, **D**, and **F**). **A:** Untreated control, showing some immunofluorescent staining in the inner border and the outer plexiform layer of the retina. **B:** Three days after detachment, SDF-1 was also expressed radially, in the border of inner retina, and some nonspecific staining was found in the photoreceptor outer segment. **C** and **D:** GFAP staining. **E** and **F:** Merged image of SDF-1 (red), GFAP (green), and DAPI (blue). Colocalization of SDF-1 and GFAP was found regardless of RD, but stronger in detached retina compared with control. INL, internal nuclear layer; ONL, outer nuclear layer. Original magnifications, $\times 200$.

rat retinal progenitor cell line.^{32,33} Cell surface expression of CXCR4 was found by immunofluorescent staining (Figure 7A). To induce cell apoptosis, we first cultured R28 cells under serum-starvation with or without SDF-1, and assessed cell survival by trypan blue dye exclusion assay after 48 hours of culturing. Serum starvation for 48 hours caused a 36.1% reduction of cell survival, compared with serum-containing medium. SDF-1 treatment dose dependently rescued serum starvation-induced cell death by 19.1% at 100 ng/ml rSDF-1 ($P < 0.05$, Figure 7B). The effect of SDF-1 was completely reversed by treatment with anti-SDF-1 antibodies (1 $\mu\text{g/ml}$; Figure 7B). TUNEL staining revealed that $11.8 \pm 6.1\%$ of cells were apoptotic after 48 hours of serum starvation. By contrast, treatment with SDF-1 significantly reduced the frequency of TUNEL-positive cells ($6.5 \pm 5.2\%$, $P < 0.05$; Figure 7, C and D). Less than 1% of the cells were TUNEL-positive with serum-containing medium. These results indicate that SDF-1 inhibits the apoptosis induced by serum starvation in R28 cells.

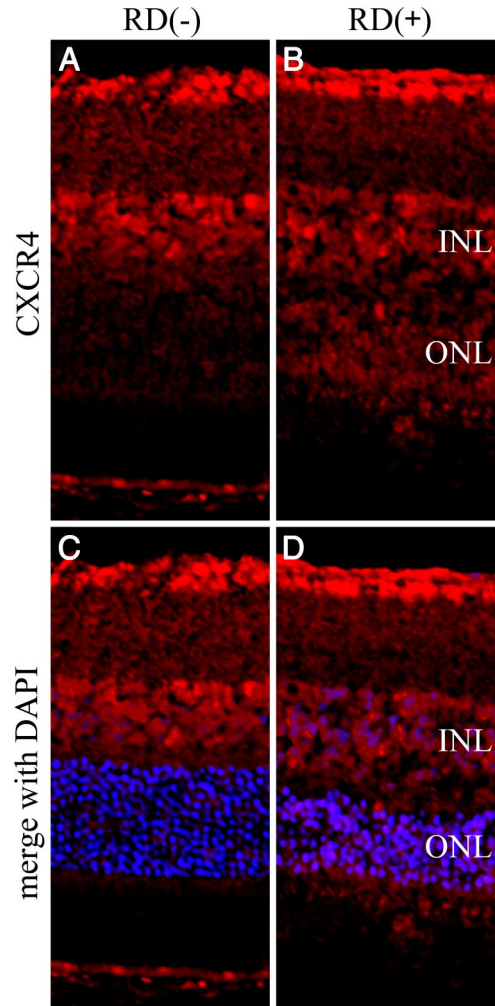


Figure 4. Confocal images of CXCR4 expression in detached rat retina. The retinal sections were derived from control eyes (**A** and **C**) or 3 days after detachment (**B** and **D**). **A:** Untreated control retina, showing positive staining in the ganglion cell layer and the inner nuclear layer of the retina. **B:** Three days after detachment, CXCR4 was strongly positive in the outer nuclear layer and photoreceptor inner segments of the detached retina. **C** and **D:** Merged images of CXCR4 (red) and DAPI (blue). INL, internal nuclear layer; ONL, outer nuclear layer. Original magnifications, $\times 200$.

SDF-1 Increases Wound Healing

To study the effects of SDF-1 on wound healing, we performed a scratch wound healing assay in the presence of SDF-1. The 90% confluent monolayers of R28

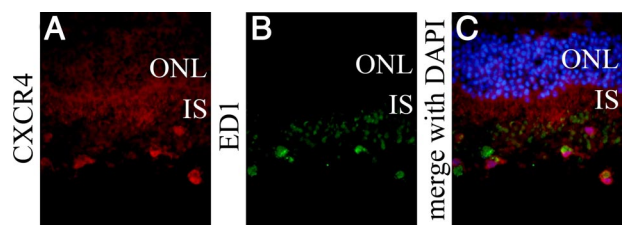


Figure 5. CXCR4 is expressed in the macrophages infiltrating into subretinal space. The retinal sections were derived at 3 days after detachment. **A:** CXCR4 staining was positive in the macrophages infiltrating into subretinal space. **B:** ED-1 stained macrophages in subretinal space. **C:** Merged image of CXCR4 (red), ED1 (green), and DAPI (blue). ONL, Outer nuclear layer; IS, inner segment. Original magnifications, $\times 400$.

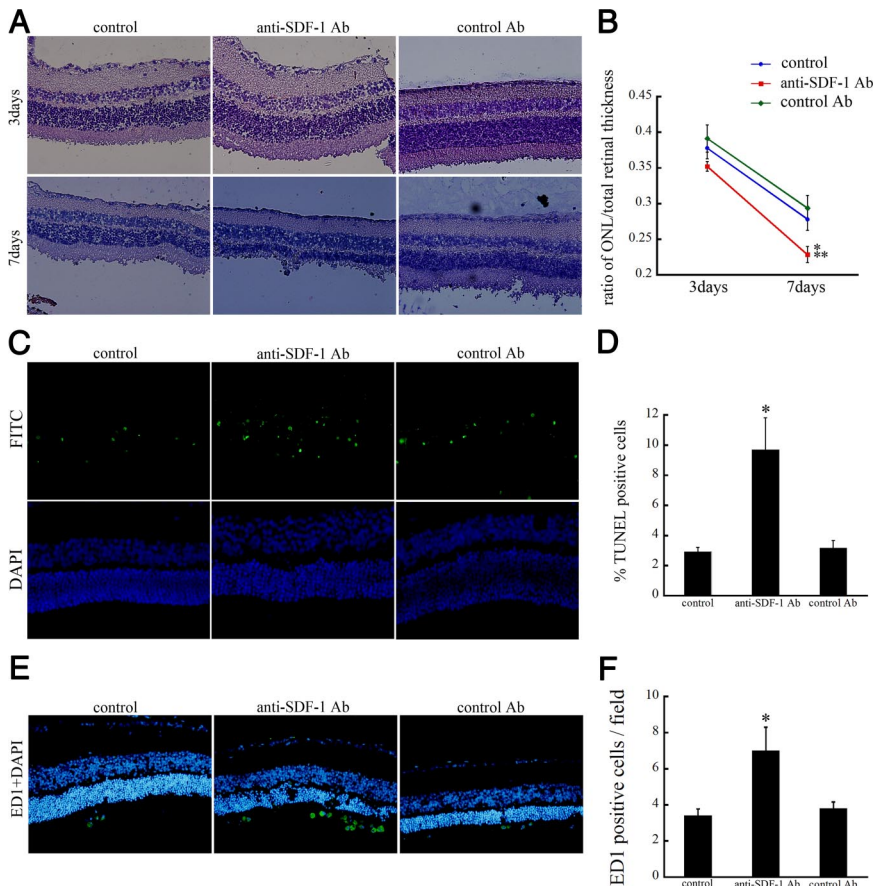


Figure 6. Effect of SDF-1 inhibition on retinal ONL thickness. Anti-SDF-1 Ab or control Ab was intravitreally injected immediately after RD induction. The rats without intravitreal injections served as controls. **A:** No apparent morphological differences among the three groups, 3 days after RD. By day 7 after RD, ONL thickness in anti-SDF-1 Ab-injected eyes was significantly lower compared with normal controls or control Ab-injected eyes. Original magnifications, $\times 200$. **B:** Graph summarizing effects of intravitreal injection on ONL thickness of rat retinas at 3 and 7 days after detachment. Results are the mean \pm SEM. $*P < 0.05$; control Ab versus anti-SDF-1 Ab injection at day 7. $**P < 0.01$; control versus anti-SDF-1 Ab injection at day 7. **C:** TUNEL staining (green) and DAPI (blue) of detached rat retinas treated with anti-SDF-1 Ab or control Ab at day 3 after RD. **D:** Quantification of TUNEL-positive cells in ONL among three groups. Results are the mean \pm SEM. $*P < 0.05$; control versus anti-SDF-1 antibody injection. **E:** Immunofluorescent staining for ED1 (green) and DAPI (blue) showing infiltrated cells into the subretinal space at day 7 after RD. Original magnifications, $\times 200$. **F:** Quantification of the number of ED1-positive macrophages among the three groups. Results are the mean \pm SEM. $*P < 0.01$; control versus anti-SDF-1 antibody injection.

cells were scratched by using a pipette tip to create a wound area. The wound area was photographed after the scratch and 24 hours later, while the cells were kept in serum-free media, containing 0.1% bovine serum albumin in the presence or absence of rSDF-1 (100 ng/ml);

Figure 8A). Subsequently, the dimensions of the healing areas were calculated (Figure 8B).

SDF-1 treatment significantly increased wound closure by 24.2% compared with control ($P < 0.01$). SDF-1's effect was reduced by the addition of anti-

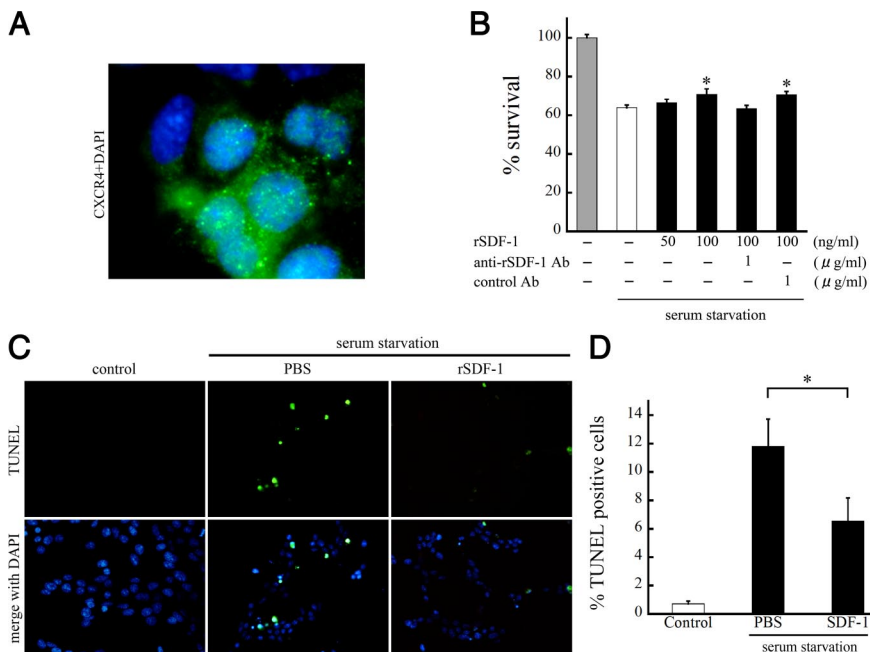


Figure 7. SDF-1 supports R28 cell survival suppressing serum starvation-induced apoptosis. **A:** Double immunofluorescent staining of CXCR4 (green) and DAPI (blue) of R28 cells. CXCR4 was predominantly expressed on the cell surface. Original magnifications, $\times 1000$. **B:** The effect of SDF-1 on cell survival. R28 cells were serum-starved and treated with PBS or rSDF-1 at the indicated doses. After 48 hours of culture, the surviving cells were counted by trypan blue dye exclusion assay ($n = 4$ each). The effect of SDF-1 was reversed by anti-SDF-1 antibody but not by control antibody. Results are the mean \pm SEM. $*P < 0.05$ versus PBS-treated control. **C** and **D:** TUNEL staining (**C**) and quantitative analysis of the TUNEL-positive apoptotic nuclei (**D**) in serum-starved R28 cells treated with PBS or rSDF-1 ($n = 4$ each). The cells growing in serum-containing medium were used as controls. Results are the mean \pm SEM. $*P < 0.05$.

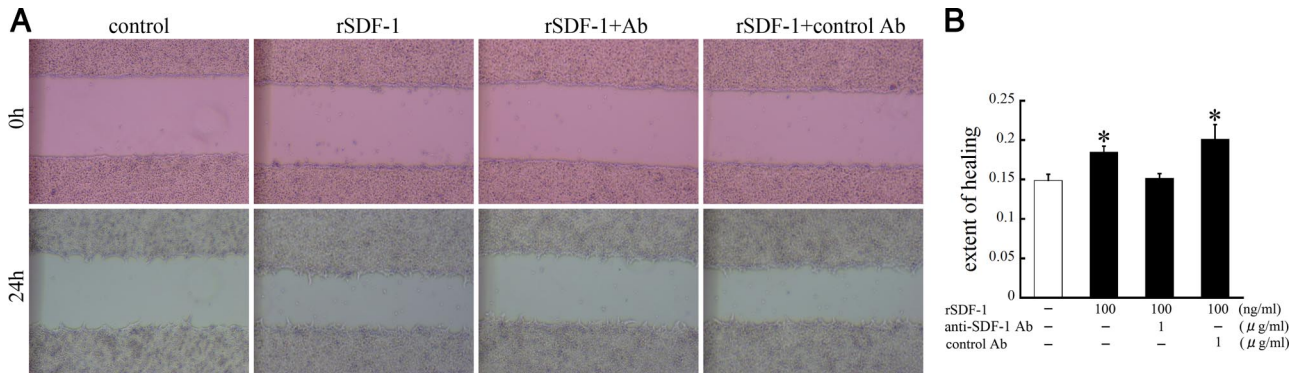


Figure 8. Effect of SDF-1 on wound healing in R28 cells. **A:** Serum-starved R28 cells at confluence were injured with a 10- μ L pipette tip. Wounded cells were allowed to heal for 24 hours in the presence or absence (control) of rSDF-1 (100 ng/ml). The extent of healing was improved by SDF-1 treatment. The effect of SDF-1 was reversed by anti-SDF-1 antibody but not by control antibody. Original magnifications, $\times 40$. **B:** Changes in the extent of healing in R28 cells. Results are the mean \pm SEM. $^*P < 0.01$; versus control.

SDF-1 Ab (0.151 \pm 0.020), but not control Ab (0.201 \pm 0.019).

SDF-1 Caused Bcl-2 Up-Regulation and ERK-1/2 Phosphorylation

To investigate the cytosolic signaling involved in survival-enhancing activity of SDF-1, we performed Western blotting by using anti-Bcl-2 antibody. The R28 cells were serum-starved and cultured with or without rSDF-1 (100 ng/ml). After 24 hours of culturing, whole cell lysates were analyzed. Western blot analysis showed increased Bcl-2 protein expression in R28 cells with SDF-1 treatment ($P < 0.01$; Figure 9, A and B).

In addition, we incubated the cells with 100 ng/ml rSDF-1 after 6 hours of serum starvation, and examined activation of signaling molecules by Western blotting by using phosphospecific antibodies. SDF-1 treatment of the R28 cells caused rapid activation of ERK1/2, which was statistically significant starting at 15 minutes ($P < 0.01$; Figure 9, C and D). The blockade of ERK signaling pathway by U0126 caused a significant reduction of Bcl-2 expression ($P < 0.01$; Figure 9, E and F).

Discussion

The present study shows the role of SDF-1 in non-neovascular ocular diseases. SDF-1 and its receptor, CXCR4, are highly expressed in the detached retina, and vitreal SDF-1 correlates with the RD pathology in patients. SDF-1 neutralization increases photoreceptor apoptosis after RD, indicating its surprising role in neuroprotection. *In vitro*, SDF-1 increases cell survival by reducing apoptosis and improving cell migration. To our knowledge, this is the first report showing increased intraocular levels of SDF-1 and its critical role in photoreceptor survival in RD.

SDF-1 has received widespread attention for its involvement in VEGF-associated ocular neovascularization, and neuroprotection through the recruitment of bone marrow-derived cells.^{9,24} For example, SDF-1 and VEGF positively correlate in diabetic retinopathy.³¹ Such a cor-

relation was also found in the PDR eyes of the present study, confirming the role of SDF-1 in the PDR pathogenesis. Previously, Butler et al¹² reported that SDF-1 is necessary and sufficient to promote proliferative retinopathy. In contrast, despite high SDF-1, significant neovas-

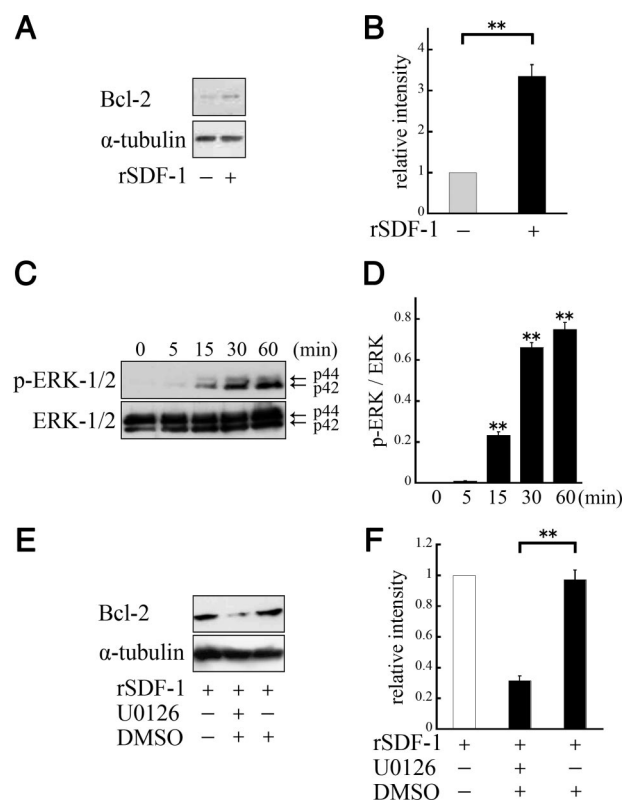


Figure 9. **A:** SDF-1 induced up-regulation of Bcl-2 protein expression. R28 cells were serum-starved and cultured with rSDF-1 (100 ng/ml) for 24 hours, and total cell lysates were analyzed by Western blot. **B:** Quantification of the relative expression of Bcl-2. Results are representative of three independent experiments, expressed as the mean \pm SEM. $^{**}P < 0.01$. **C:** SDF-1 induced the phosphorylation of ERK. R28 cells were stimulated with rSDF-1 (100 ng/ml) for 5, 15, 30, or 60 minutes. **D:** Quantification of p-ERK/ERK ratio. Results are representative of three independent experiments, expressed as the mean \pm SEM. $^{**}P < 0.01$; versus control. **E:** ERK signaling was essential to the regulation of Bcl-2. After 3 hours of serum starvation, U0126 was applied 1 hour before SDF-1 treatment. **F:** Quantification of the relative expression of Bcl-2. $^{**}P < 0.01$; versus dimethyl sulfoxide.

cularization or proliferative retinopathy was not found in our RD eyes.¹² Our results indicate that SDF-1 alone is not sufficient to promote proliferative retinopathy, suggesting that in addition to high SDF-1, VEGF, ischemic injury, or other factors might be necessary to promote proliferative retinopathy in humans. The positive correlation of SDF-1 with disease duration, as well as the extent of the detached retina, indicates that SDF-1 is produced by the detached retina or a related event. SDF-1 was also positively correlated with IL-6, a protective factor in RD,²¹ suggesting that part of SDF-1's action might be through other factors. These clinical data indicate SDF-1 to be a key player in RD pathology.

In our study, although RD shows the highest vitreous SDF-1 levels among the studied conditions, VEGF levels in RD are low. However, considering outer retinal ischemia,³⁴ the VEGF level was also expected to be high. Possible explanations of this discrepancy are as follows: (1) there are undetectable levels of VEGF production; (2) VEGF is released predominantly into subretinal space in RD. Further studies will be required to elucidate this point.

In ocular diseases, SDF-1 is induced by ischemia.^{35,36} Retinal glia,³⁵ as well as endothelial cells, releases SDF-1.³⁶ SDF-1 colocalizes in the inner retina with GFAP-expressing cells in normal and detached retinas, suggesting SDF-1 production in glial cells, such as Müller cells, astrocytes, and microglia. Up-regulation of GFAP-positive glia is found in relation to central nervous system stress, including RD.^{37,38} Therefore, it appears likely that SDF-1 is released by reactive retinal glia in RD. In RD, the inner retina is believed to be sufficiently supplied by retinal circulation so that ischemia generally does not occur,³⁴ suggesting that other stimuli besides ischemia might be responsible for SDF-1 up-regulation.

SDF-1 blockade causes a significant accumulation of inflammatory cells in the subretinal space and photoreceptor loss after RD. This is in line with the finding that SDF-1 blockade aggravates retinal degeneration in C3H/HeJ (rd1/rd1) mice.²⁴ SDF-1 rescues serum starvation-induced apoptosis of R28 cells dose-dependently, possibly through bcl2 up-regulation and activation of the ERK-pathway. This is in line with a previous report that SDF-1 suppresses apoptosis of cultured dendritic cells.³⁹

SDF-1 stimulates the wound-healing response in R28 cells. Because SDF-1 is up-regulated both in the animal model of RD and in samples from patients with RD, it is reasonable to assume that SDF-1 is part of the organ's response to minimize injury, and that blocking it would enhance retinal damage.

Sasahara et al²⁴ reported that SDF-1 blockade decreases the accumulation of neuro-protective bone marrow-derived microglial cells, resulting in progression of retinal degeneration. Our results show accumulation of CXCR4-positive macrophages around the retinal vessels and in the subretinal spaces, suggesting that SDF-1 acts as a chemo-attractant for inflammatory cells in RD. However, accumulation of subretinal macrophages increased significantly in the SDF-1-blocked eyes, differing from the results by Sasahara et al²⁴ in the retinal degeneration

model. An explanation for this discrepancy could be that in RD, the retina is damaged acutely and more severely than in the chronic retinal degeneration model. As a result, the mediators of cell damage might differ between RD and retinal degeneration. For instance, damage-associated molecular pattern molecules, strong chemo-attractants for inflammatory cells, are produced after injury,^{40,41} and we found the damage-associated molecular pattern molecule member, the high-mobility group box-1, subretinally in RD.²³

The fact that SDF-1 blockade increases damage in detached retinas suggests that SDF-1 might limit the production of chemical mediators of injury, including damage-associated molecular pattern molecules. This might also explain the increased accumulation of inflammatory cells in the subretinal space of RD eyes with SDF-1 blockade.

Interestingly, SDF-1 blockade affects the detached but not the normal retina, suggesting that the detached-retina is more sensitive to environmental changes than the normal retina. This tendency was also described in RD of IL-6^{-/-} mice.²¹ SDF-1 blockade has been proposed as a new therapeutic strategy for proliferative ocular diseases.¹² However, proliferative diseases are often associated with RD, so anti-SDF-1 therapy might be counter-indicated.

Anti-VEGF agents have recently shown therapeutic success in age-related macular degeneration and diabetic retinopathy.⁴² Intraocular mediators of inflammation and angiogenesis build a complex network, and targeting one of them affects various others. We showed that VEGF inhibition decreases SDF-1 in the eye.²³ This might explain some of the deleterious effects of anti-VEGF therapy and indicate the need for careful consideration of the indication for VEGF-targeting with respect to RD.

In sum, SDF-1 has both beneficial and adverse effects in RD, such as neuro-protection or inflammatory cell accumulation, respectively. Endogenous SDF-1 is tissue-protective in RD. Elucidating the detailed mechanisms underlying SDF-1's role in neural protection will support the development of safe and effective treatments.

References

- Schall TJ: Biology of the RANTES/SIS cytokine family. *Cytokine* 1991, 3:165-183
- Oppenheim JJ, Zachariae CO, Mukaida N, Matsushima K: Properties of the novel proinflammatory supergene "intercrine" cytokine family. *Annu Rev Immunol* 1991, 9:617-648
- Luster AD: Chemokines—chemotactic cytokines that mediate inflammation. *N Engl J Med* 1998, 338:436-445
- Schall TJ, Bacon KB: Chemokines, leukocyte trafficking, and inflammation. *Curr Opin Immunol* 1994, 6:865-873
- Nagasawa T, Hirota S, Tachibana K, Takakura N, Nishikawa S, Kitamura Y, Yoshida N, Kikutani H, Kishimoto T: Defects of B-cell lymphopoiesis and bone-marrow myelopoiesis in mice lacking the CXC chemokine PBSF/SDF-1. *Nature* 1996, 382:635-638
- Lazarini F, Tham TN, Casanova P, Arenzana-Seisdedos F, Dubois-Dalq M: Role of the alpha-chemokine stromal cell-derived factor (SDF-1) in the developing and mature central nervous system. *Glia* 2003, 42:139-148
- Burger JA, Kipps TJ: CXCR4: a key receptor in the crosstalk between tumor cells and their microenvironment. *Blood* 2006, 107:1761-1767

8. Lataillade JJ, Clay D, Dupuy C, Rigal S, Jasmin C, Bourin P, Le Bousse-Kerdiles MC: Chemokine SDF-1 enhances circulating CD34(+) cell proliferation in synergy with cytokines: possible role in progenitor survival. *Blood* 2000, 95:756–768
9. Ruiz de Almodovar C, Luttun A, Carmeliet P: An SDF-1 trap for myeloid cells stimulates angiogenesis. *Cell* 2006, 124:18–21
10. Askari AT, Unzek S, Popovic ZB, Goldman CK, Forudi F, Kiedrowski M, Rovner A, Ellis SG, Thomas JD, DiCorleto PE, Topol EJ, Penn MS: Effect of stromal-cell-derived factor 1 on stem-cell homing and tissue regeneration in ischaemic cardiomyopathy. *Lancet* 2003, 362:697–703
11. Sengupta N, Caballero S, Mames RN, Butler JM, Scott EW, Grant MB: The role of adult bone marrow-derived stem cells in choroidal neovascularization. *Invest Ophthalmol Vis Sci* 2003, 44:4908–4913
12. Butler JM, Guthrie SM, Koc M, Afzal A, Caballero S, Brooks HL, Mames RN, Segal MS, Grant MB, Scott EW: SDF-1 is both necessary and sufficient to promote proliferative retinopathy. *J Clin Invest* 2005, 115:86–93
13. Sonmez K, Drenser KA, Capone A Jr, Trese MT: Vitreous levels of stromal cell-derived factor 1 and vascular endothelial growth factor in patients with retinopathy of prematurity. *Ophthalmology* 2008, 115:1065–1070
14. Ki IY, Arimura N, Noda Y, Yamakiri K, Doi N, Hashiguchi T, Maruyama I, Shimura M, Sakamoto T: Stromal-derived factor-1 and inflammatory cytokines in retinal vein occlusion. *Curr Eye Res* 2007, 32:1065–1072
15. Curnow SJ, Wloka K, Faint JM, Amft N, Cheung CM, Savant V, Lord J, Akbar AN, Buckley CD, Murray PI, Salmon M: Topical glucocorticoid therapy directly induces up-regulation of functional CXCR4 on primed T lymphocytes in the aqueous humor of patients with uveitis. *J Immunol* 2004, 172:7154–7161
16. Abu El-Asrar AM, Struyf S, Kangave D, Geboes K, Van Damme J: Chemokines in proliferative diabetic retinopathy and proliferative vitreoretinopathy. *Eur Cytokine Netw* 2006, 17:155–165
17. Cook B, Lewis GP, Fisher SK, Adler R: Apoptotic photoreceptor degeneration in experimental retinal detachment. *Invest Ophthalmol Vis Sci* 1995, 36:990–996
18. Yang L, Bula D, Arroyo JG, Chen DF: Preventing retinal detachment-associated photoreceptor cell loss in Bax-deficient mice. *Invest Ophthalmol Vis Sci* 2004, 45:648–654
19. Arroyo JG, Yang L, Bula D, Chen DF: Photoreceptor apoptosis in human retinal detachment. *Am J Ophthalmol* 2005, 139:605–610
20. Digicaylioglu M, Lipton SA: Erythropoietin-mediated neuroprotection involves cross-talk between Jak2 and NF-kappaB signalling cascades. *Nature* 2001, 412:641–647
21. Chong DY, Boehlke CS, Zheng QD, Zhang L, Han Y, Zacks DN: Interleukin-6 as a photoreceptor neuroprotectant in an experimental model of retinal detachment. *Invest Ophthalmol Vis Sci* 2008, 49:3193–3200
22. Nakazawa T, Hisatomi T, Nakazawa C, Noda K, Maruyama K, She H, Matsubara A, Miyahara S, Nakao S, Yin Y, Benowitz L, Hafezi-Moghadam A, Miller JW: Monocyte chemoattractant protein 1 mediates retinal detachment-induced photoreceptor apoptosis. *Proc Natl Acad Sci USA* 2007, 104:2425–2430
23. Arimura N, Otsuka H, Yamakiri K, Sonoda Y, Nakao S, Noda Y, Hashiguchi T, Maruyama I, Sakamoto T: Vitreous mediators after intravitreal bevacizumab or triamcinolone acetonide in eyes with proliferative diabetic retinopathy. *Ophthalmology* 2009, 116:921–926
24. Sasahara M, Otani A, Oishi A, Kojima H, Yodoi Y, Kameda T, Nakamura H, Yoshimura N: Activation of bone marrow-derived microglia promotes photoreceptor survival in inherited retinal degeneration. *Am J Pathol* 2008, 172:1693–1703
25. Xie Z, Wu X, Qiu Q, Gong Y, Song Y, Gu Q, Li C: Expression pattern of erythropoietin and erythropoietin receptor in experimental model of retinal detachment. *Curr Eye Res* 2007, 32:757–764
26. Neekhra A, Luthra S, Chwa M, Seigel G, Gramajo AL, Kuppermann BD, Kenney MC: Caspase-8, -12, and -3 activation by 7-ketocholesterol in retinal neurosensory cells. *Invest Ophthalmol Vis Sci* 2007, 48:1362–1367
27. Sareen D, van Ginkel PR, Takach JC, Mohiuddin A, Darjatmoko SR, Albert DM, Polans AS: Mitochondria as the primary target of resveratrol-induced apoptosis in human retinoblastoma cells. *Invest Ophthalmol Vis Sci* 2006, 47:3708–3716
28. Xu KP, Yu FS: Cross talk between c-Met and epidermal growth factor receptor during retinal pigment epithelial wound healing. *Invest Ophthalmol Vis Sci* 2007, 48:2242–2248
29. Murakami Y, Ikeda Y, Yonemitsu Y, Onimaru M, Nakagawa K, Kohno R, Miyazaki M, Hisatomi T, Nakamura M, Yabe T, Hasegawa M, Ishibashi T, Sueishi K: Inhibition of nuclear translocation of apoptosis-inducing factor is an essential mechanism of the neuroprotective activity of pigment epithelium-derived factor in a rat model of retinal degeneration. *Am J Pathol* 2008, 173:1326–1338
30. Arimura N, Ki-i Y, Hashiguchi T, Kawahara K, Biswas KK, Nakamura M, Sonoda Y, Yamakiri K, Okubo A, Sakamoto T, Maruyama I: Intraocular expression and release of high-mobility group box 1 protein in retinal detachment. *Lab Invest* 2009, 89:278–289
31. Brooks HL Jr, Caballero S Jr, Newell CK, Steinmetz RL, Watson D, Segal MS, Harrison JK, Scott EW, Grant MB: Vitreous levels of vascular endothelial growth factor and stromal-derived factor 1 in patients with diabetic retinopathy and cystoid macular edema before and after intraocular injection of triamcinolone. *Arch Ophthalmol* 2004, 122:1801–1807
32. Seigel GM, Sun W, Wang J, Hershberger DH, Campbell LM, Salvi RJ: Neuronal gene expression and function in the growth-stimulated R28 retinal precursor cell line. *Curr Eye Res* 2004, 28:257–269
33. Seigel GM, Mutchler AL, Adams G, Imperato-Kalmar EL: Recoverin expression in the R28 retinal precursor cell line. *In Vitro Cell Dev Biol Anim* 1997, 33:499–502
34. Wang S, Linsenmeier RA: Hyperoxia improves oxygen consumption in the detached feline retina. *Invest Ophthalmol Vis Sci* 2007, 48:1335–1341
35. Lima e Silva R, Shen J, Hackett SF, Kachi S, Akiyama H, Kiuchi K, Yokoi K, Hatara MC, Lauer T, Aslam S, Gong YY, Xiao WH, Khu NH, Thut C, Campochiaro PA: The SDF-1/CXCR4 ligand/receptor pair is an important contributor to several types of ocular neovascularization. *FASEB J* 2007, 21:3219–3230
36. Lai P, Li T, Yang J, Xie C, Zhu X, Xie H, Ding X, Lin S, Tang S: Upregulation of stromal cell-derived factor 1 (SDF-1) expression in microvasculature endothelial cells in retinal ischemia-reperfusion injury. *Graefes Arch Clin Exp Ophthalmol* 2008, 246:1707–1713
37. Nakazawa T, Takeda M, Lewis GP, Cho KS, Jiao J, Wilhelmsson U, Fisher SK, Pekny M, Chen DF, Miller JW: Attenuated glial reactions and photoreceptor degeneration after retinal detachment in mice deficient in glial fibrillary acidic protein and vimentin. *Invest Ophthalmol Vis Sci* 2007, 48:2760–2768
38. Lewis GP, Fisher SK: Up-regulation of glial fibrillary acidic protein in response to retinal injury: its potential role in glial remodeling and a comparison to vimentin expression. *Int Rev Cytol* 2003, 230:263–290
39. Hernandez-Lopez C, Valencia J, Hidalgo L, Martinez VG, Zapata AG, Sacedon R, Varas A, Vicente A: CXCL12/CXCR4 signaling promotes human thymic dendritic cell survival regulating the Bcl-2/Bax ratio. *Immunol Lett* 2008, 120:72–78
40. Yang D, Chen Q, Yang H, Tracey KJ, Bustin M, Oppenheim JJ: High mobility group box-1 protein induces the migration and activation of human dendritic cells and acts as an alarmin. *J Leukoc Biol* 2007, 81:59–66
41. Abraham E, Arcaroli J, Carmody A, Wang H, Tracey KJ: HMG-1 as a mediator of acute lung inflammation. *J Immunol* 2000, 165:2950–2954
42. Rosenfeld PJ, Brown DM, Heier JS, Boyer DS, Kaiser PK, Chung CY, Kim RY: Ranibizumab for neovascular age-related macular degeneration. *N Engl J Med* 2006, 355:1419–1431